Endogenously Nitrated Proteins in Mouse Brain: Links to Neurodegenerative Disease†

Colette A. Sacksteder,‡,§ Wei-Jun Qian,§,|| Tatyana V. Knyushko,‡ Haixing Wang,|| Mark H. Chin,⊥ Goran Lacan,@ William P. Melega,@ David G. Camp, II,|| Richard D. Smith,|| Desmond J. Smith,@ Thomas C. Squier,‡ and Diana J. Bigelow*,‡

Cell Biology and Biochemistry Group and Biological Science Division, Pacific Northwest National Laboratory, Richland, Washington 99352, and Department of Human Genetics and Department of Molecular and Medical Pharmacology, David Geffen School of Medicine at UCLA, Los Angeles, California 90095

Received March 9, 2006; Revised Manuscript Received May 9, 2006

ABSTRACT: Increased abundance of nitrotyrosine modifications of proteins have been documented in multiple pathologies in a variety of tissue types and play a role in the redox regulation of normal metabolism. To identify proteins sensitive to nitrating conditions in vivo, a comprehensive proteomic data set identifying 7792 proteins from a whole mouse brain, generated by LC/LC−MS/MS analyses, was used to identify nitrated proteins. This analysis resulted in the identification of 31 unique nitrotyrosine sites within 29 different proteins. More than half of the nitrated proteins that have been identified are involved in Parkinson's disease, Alzheimer's disease, or other neurodegenerative disorders. Similarly, nitrotyrosine immunoblots of whole brain homogenates show that treatment of mice with 1-methyl-4-phenyl-1,2,3,6-tetrahydropyridine (MPTP), an experimental model of Parkinson's disease, induces an increased level of nitration of the same protein bands observed to be nitrated in brains of untreated animals. Comparing sequences and available high-resolution structures around nitrated tyrosines with those of unmodified sites indicates a preference of nitration in vivo for surface accessible tyrosines in loops, a characteristic consistent with peroxynitrite-induced tyrosine modification. In addition, most sequences contain cysteines or methionines proximal to nitrotyrosines, contrary to suggestions that these amino acid side chains prevent tyrosine nitration. More striking is the presence of a positively charged moiety near the sites of nitration, which is not observed for non-nitrated tyrosines. Together, these observations suggest a predictive tool of functionally important sites of nitration and that cellular nitrating conditions play a role in neurodegenerative changes in the brain.

Increased levels of 3-nitrotyrosine modification of proteins has been observed in more than 80 different oxidative stress and inflammation-related pathologies; in the case of coronary artery disease, nitrotyrosine is as reliable as C-reactive protein as a biomarker (*1*, *2*). In several cases, specific nitrated proteins and their associated dysfunctions have been identified, providing insight into the molecular mechanisms of disease. Although considerably less is understood with regard to structural consequences, nitration can affect enzyme catalytic rates, protein−protein interactions, and phosphotyrosine signaling pathways (*3*−*9*). The appearance of nitrated proteins in tissues may arise from nitric oxide-derived oxidation products such as nitrogen dioxide ($^{\bullet}NO_2$), peroxynitrite ($ONOO^-$), or its CO_2 adduct, nitrosoperoxocarbonate (*10*−*12*). Peroxynitrite is formed by the spontaneous combination of nitric oxide ($NO^{\bullet}$) with superoxide ($O_2^{-\bullet}$); the near-diffusion-controlled rate of this reaction permits efficient competition of nitric oxide with superoxide dismutase, which normally detoxifies cellular superoxide (*10*). Thus, cellular conditions that result in elevated nitric oxide levels, such as inflammation with induction of nitric oxide synthase (NOS2) or superoxide generation from defective mitochondrial respiration, are likely to lead to an increased level of protein nitration (*13*). An additional source of protein nitration is the reaction of hydrogen peroxide and nitrite mediated by heme peroxidases in macrophages and neutrophils (*14*).

In addition to its role in cellular damage and disease, recent work has suggested that tyrosine nitration can serve in a regulatory role; reversible nitration, in response to redox

† This work was supported by grants from the National Institutes of Health [AG18013 and AG12993 (D.J.B. and T.C.S.), RR018522 (R.D.S.), NS050148 (D.J.S. and R.D.S.), and DA015802 (D.J.S.)] and the LDRD Program at the Pacific Northwest National Laboratory, a multiprogram national laboratory operated by Battelle for the U.S. Department of Energy under Contract DE-AC06-76RL01830. The Environmental Molecular Sciences Laboratory (EMSL) provided analytical instrumentation.

* To whom correspondence should be addressed: Pacific Northwest National Laboratory, P.O. Box 999, MS P7-56, Richland, WA 99352. E-mail: diana.bigelow@pnl.gov. Telephone: (509) 376-2378. Fax: (509) 376-6767.

‡ Cell Biology and Biochemistry Group, Pacific Northwest National Laboratory.

§ These authors contributed equally to this work.

|| Biological Science Division, Pacific Northwest National Laboratory.

⊥ Department of Human Genetics, David Geffen School of Medicine at UCLA.

@ Department of Molecular and Medical Pharmacology, David Geffen School of Medicine at UCLA.

10.1021/bi060474w CCC: $33.50
Published on Web 06/08/2006

conditions, has been demonstrated in mitochondria for proteins critical for energy and antioxidant homeostasis (*15*). Moreover, peroxynitrite, itself, has been shown to act as an intermediate in nitric oxide-induced relaxation of smooth muscle through glutathiolation of a critical cysteine within SERCA (*16*). However, at higher peroxynitrite concentrations, relaxation is disrupted by irreversible oxidation of cysteine with the appearance of tyrosine nitration, simulating the oxidation status and functional deficits observed in atherosclerosis. Together, these new studies suggest an emerging picture of peroxynitrite and its protein oxidation products playing diverse roles in the regulation of cellular processes that are responsive to nitric oxide and reactive oxygen, with excessive levels resulting in irreversible dysfunction. Therefore, proteins sensitive to modification by reactive nitrogen species may be involved in redox regulation or represent sites of cellular vulnerability under conditions of nitrative stress.

In this study, we have examined the proteome of normal mouse brain to identify nitrotyrosine-modified proteins and their relative stoichiometries that are present in vivo under nonstressed conditions. Such endogenously nitrated proteins were identified using high-resolution separation of tryptic peptides coupled with tandem mass spectrometric analysis. From a global screen identifying 7792 proteins, 29 (0.4%) nitrated proteins were identified with very high confidence from MS/MS[1] fragmentation spectra. More than half of these nitrated proteins have been shown previously to have functional links with Parkinson's disease (PD) or other neurodegenerative diseases, suggesting that proteins that are normally regulated or otherwise sensitive to nitration are more extensively nitrated during the progression of neurodegenerative disorders. Analysis of this data set of nitrated tyrosine peptides compared with non-nitrated tyrosine-containing peptides demonstrates a striking preference for proximal basic amino acids that may be predictive of nitration sensitive tyrosines.

MATERIALS AND METHODS

Animals and Treatment. C57BL/6J mice, obtained from Jackson Laboratories (Bar Harbor, ME), were housed three per cage in a temperature-controlled room under a 12 h light−dark cycle with free access to food and water. On the day of the experiment, mice received four intraperitoneal injections of MPTP-HCl (Sigma) in saline (15 mg/kg of body weight) at 2 h intervals; control mice received saline only. Six days later, mice were sacrificed after deep anesthesia with isoflurane. The brains were removed and immediately frozen on dry ice until they were analyzed. Results of HPLC analysis of striatal homogenates indicated that the MPTP treatment regimen used in this study induced a 60% loss of dopamine content in the striatum 6 days following the treatment (80.3 ± 6.5 ng/mg of protein in lesioned animals vs 200 ± 28.0 ng/mg of protein in controls; $p < 0.0002$, 12 d.f., using the Student's *t*-test). All tissue was from 9-week-old mice.

HPLC Analysis of Striatal Samples. The contents of dopamine (DA) and its metabolites were determined with HPLC. Mice striatal tissues were homogenized by sonication in 0.5 mL of ice-cold 0.2 M $HClO_4$ containing 0.15% (w/v) Na_2EDTA and centrifuged at 14 000 rpm for 15 min (4 °C), prior to filtration of the supernatant through 0.2 μm PTFE. HPLC analysis of a 20 μL aliquot was carried out with a reversed phase Adsorbosphere HS C18 column (100 mm × 4.6 mm, 3 μm, Alltech) with a guard column (7.5 mm × 4.6 mm, 5 μm) and an electrochemical detector (ESA Coulochem II, model 5011 analytical cell). The analytical cell was operated at 350 mV and 500 nA. The mobile phase consisted of acetonitrite and sodium phosphate buffer [75 mM $NaH_2PO_4 \cdot H_2O$, 1.8 mM 1-octanesulfonic acid sodium salt monohydrate, and 12 μM EDTA (pH 3.1)] at a 6.5:93.5 (v/v) ratio. The flow rate was 0.8 mL/min. Analytes were quantified by reference to respective standards. The detector response was linear from 0.05 to 10 ng ($r = 0.99$ for linear regression calculations for all compounds assayed; within-assay and between-assay variance was <3−5%).

Immunoblots of Mouse Brain Homogenates. Whole brain tissues from untreated and MPTP-stimulated mice (C57BL/6J) were each sliced into small pieces (~20 mg each) and placed into individual tubes containing 250 μL of 0.5% SDS and 50 mM NH_4HCO_3 (pH 7.8). Samples were homogenized by vortexing followed by sonication in an ice−water bath; pooled homogenates for each mouse brain were assayed for protein concentration by the Coomassie protein assay (Pierce, Rockford, IL). Proteins in each sample were electrophoretically separated by SDS−PAGE using a 4 to 12% gradient polyacrylamide gel and MES running buffer (Invitrogen, Carlsbad, CA) prior to transfer (1.5 h at 30 V) to a PVDF membrane. For detection of nitrated proteins, blots were probed with anti-3-nitrotyrosine monoclonal antibody (clone 1A2-9, gift from J. S. Beckman, Oregon State University, Corvallis, OR) or a polyclonal antibody (Biodesign, Saco, ME), using a dilution of 1:100 or 1:10000, respectively. Final visualization required appropriate secondary antibodies conjugated with horseradish peroxidase for detection with SuperSignal West Femto Maximum Sensitivity Substrate (Pierce).

Mass Spectrometry of Brain Peptides. Tryptic peptides were prepared as described previously (*17*). Briefly, small pieces of frozen brain were vortexed in 5 mM sodium phosphate (pH 7.0), followed by sonication for 5 min in an ice−water bath. For denaturation and reduction, each sample was incubated for 1 h at 60 °C in a 1:1 mixture of trifluoroethanol and 5 mM tributylphosphine. After 5-fold dilution with 5 mM NH_4HCO_3 (pH 7.8), samples were digested with addition of sequencing-grade modified trypsin (Promega, Madison, WI), at a ratio of 1:50 (w/w, enzyme:protein), incubating at 37 °C overnight with gentle shaking. The resulting peptides were desalted using a 1 mL SPE C18 column (Supelco, Bellefonte, PA), eluting with an 80% acetonitrile/0.1% TFA solution prior to lyophilization of the eluted peptides. Protein concentrations were measured using the bicinchoninic acid (BCA) protein assay (Pierce).

Cysteinyl-Peptide Enrichment (CPE). Approximately 5 mg of the tryptic digests was fractionated for cysteinyl-peptide enrichment, as previously described (*17*). Briefly, peptides were lyophilized and then redissolved in 120 μL of coupling buffer which consisted of 50 mM Tris-HCl (pH 7.5) and 1

[1] Abbreviations: AD, Alzheimer's disease; GO, gene ontology; LC, liquid chromatography; MPTP, 1-methyl-4-phenyl-1,2,3,6-tetrahydropyridine; MS, mass spectrometry; NCBI, National Center for Bioinformatics Institute; NY, nitrotyrosine; PD, Parkinson's disease; SCX, strong cation exchange; SDS−PAGE, sodium dodecyl sulfate−polyacrylamide gel electrophoresis; TH, tyrosine hydroxylase.

mM EDTA. Freshly made dithiothreitol (DTT) was added at 5 mM to reduce the sample, with incubation for 1 h at 37 °C. Subsequently, the sample was diluted to 600 μL with coupling buffer prior to their application, as four equal aliquots, to a Handee Mini-spin column (Pierce) containing 100 μL of thiopropyl-Sepharose 6B resin (Amersham, Piscataway, NJ) followed by a 2 h incubation with gentle shaking at room temperature. Unbound peptides were removed by stringent washing with 50 mM Tris buffer, 2 M NaCl, and an 80% acetonitrile/0.1% TFA solution. Cysteinyl-peptides were eluted with 120 μL of 20 mM freshly made DTT incubating at room temperature for 30 min. The released peptides were carboxamidomethylated with 40 mM iodoacetamide for 1 h at room temperature in the dark. Alkylated peptide samples were then desalted using a 1 mL SPE C18 column. After lyophilization, peptides were resuspended in 600 μL of 10 mM ammonium formate (Sigma, St. Louis, MO) in 25% acetonitrile (pH 3.0) for strong cation exchange (SCX) fractionation.

Strong Cation Exchange (SCX) Fractionation. Both the global tryptic peptides and enriched cysteinyl-peptides were subjected to an HPLC fractionation by SCX chromatography on a Polysulfoethyl A column (200 mm × 2.1 mm) (PolyLC, Columbia, MD) preceded by a 10 mm × 2.1 mm guard column with a flow rate of 0.2 mL/min. Separations were performed with an Agilent 1100 series HPLC system (Agilent) with mobile phases consisting of solvent A [10 mM ammonium formate and 25% acetonitrile (pH 3.0)] and solvent B [500 mM ammonium formate and 25% acetonitrile (pH 6.8)]. Once the column was loaded, the run was isocratic for 10 min at 100% A. Peptides were separated with a gradient from 0 to 50% B over the course of 40 min, followed by a gradient from 50 to 100% B over the course of 10 min, and finally with 100% solvent B for 10 min. Thirty fractions each were collected for both the global peptide sample and the enriched cysteinyl-peptide sample. Following lyophilization, the fractions were dissolved in 25 mM NH_4HCO_3 and stored at −80 °C until they were analyzed.

Capillary LC−MS/MS Analysis. Each of the 30 SCX fractions from both global digests and enriched cysteinyl-peptides was further analyzed using a fully automated custom-built capillary HPLC system coupled online with an LTQ ion trap mass spectrometer (ThermoFinnigan, San Jose, CA) using an in-house manufactured electrospray ionization interface. The reversed phase capillary column was slurry packed using 3 μm Jupiter C_{18} particles (Phenomenex, Torrance, CA) into a 150 μm (inside diameter) × 65 cm fused silica capillary (Polymicro Technologies, Phoenix, AZ). The mobile phases consisted of A (0.2% acetic acid and 0.05% TFA in water) and B (0.1% TFA in 90% acetonitrile). An exponential gradient was employed in the separation, which started with 100% A and gradually increased to 60% B over the course of 100 min. The instrument was operated in data-dependent mode with an *m*/*z* range of 400−2000. The five most abundant ions from MS analysis were selected for further MS/MS analysis using a normalized collision energy setting of 35%. Dynamic exclusion was used to avoid repetitive analysis of the same abundant precursor ion.

MS/MS Data Analysis. The MS/MS data were searched against the mouse International Protein Index (IPI) database (version 1.25, available at http://ebi.ac.uk/IPI) and a sequence-reversed IPI database (to assess false positives) using SEQUEST (Thermo Finnigan). For enriched cysteinyl-peptide samples, static carboxymethylation modification (57.0215 Da) was applied on cysteine residues. For identification of methionine sulfoxides and 3-nitrotyrosines, dynamic modifications of 15.9949 and 44.9851 Da were applied on the methionine and tyrosine residues, respectively. The following criteria were used for initial filtering of the raw SEQUEST results: Xcorr ≥ 1.6 for the +1 charge state full tryptic peptides, Xcorr ≥ 2.4 for the +2 charge state full tryptic peptides, Xcorr ≥ 4.3 for partial tryptic peptides, Xcorr ≥ 3.2 for the +3 charge state full tryptic peptides, and Xcorr ≥ 4.7 for partial tryptic peptides for which $\Delta C_n > 0.1$. Such criteria were established for mouse brain tissue using sequence-reversed database searching that provides <2% of false positive peptide identifications (*18*). To remove redundant protein entries, ProteinProphet was used as a clustering tool to group similar or related protein entries (*19*). To increase the confidence level of nitrotyrosine peptide identifications, additional constraints were applied, including (i) the presence of a cysteine residue for all nitrated peptides identified from cysteinyl-peptide enriched samples, (ii) the fact that for peptides identified from the global peptide sample, there is retention of peptides without cysteinyl residues, and (iii) manual inspection of all remaining peptide identifications at the MS/MS spectrum level to ensure that major MS/MS fragmentation peaks matched their theoretical predictions. Following inspection, 36 peptides were determined to be confident nitrotyrosine identifications.

Spatial Locations. Cellular locations for identified proteins were obtained using the FatiGO web tool (*20*) (http://www.fatigo.org/) for the association of genes with Gene Ontology (GO) terms (http://www.geneontology.org/). NCBI gene symbols were obtained for each International Protein Index (IPI) number (http://www.ebi.ac.uk/IPI/xrefs.html).

RESULTS

Brain Proteins Identified from a Global Proteomic Screen. The identification of endogenously nitrated brain proteins utilized a global proteomic strategy (two-dimensional LC−MS/MS) that permits the sensitive detection of both modified peptides and their native analogues from the same complex cellular mixtures, thus providing a semiquantitative estimate of their relative stoichiometries in vivo. Therefore, tryptic peptides from whole brain homogenates were fractionated prior to LC−MS/MS identification, an experimental approach that has been demonstrated to provide reproducible and sensitive identification of membrane as well as soluble peptides and proteins (*21*). As an additional means of enhancing proteome detection, a portion of the tryptic peptides was subjected to cysteinyl-peptide enrichment prior to cysteine alkylation (*17*). The remaining (global) portion was analyzed without cysteine alkylation, essentially depleting this portion of cysteinyl-peptides to provide a complementary sample to the cysteinyl-enriched peptides. Both portions were fractionated in parallel by strong cation exchange chromatography (SCX), and the 30 resulting peptide fractions were each analyzed by high-resolution capillary LC−MS/MS. The MS/MS data were searched against the mouse International Protein Index (IPI) database

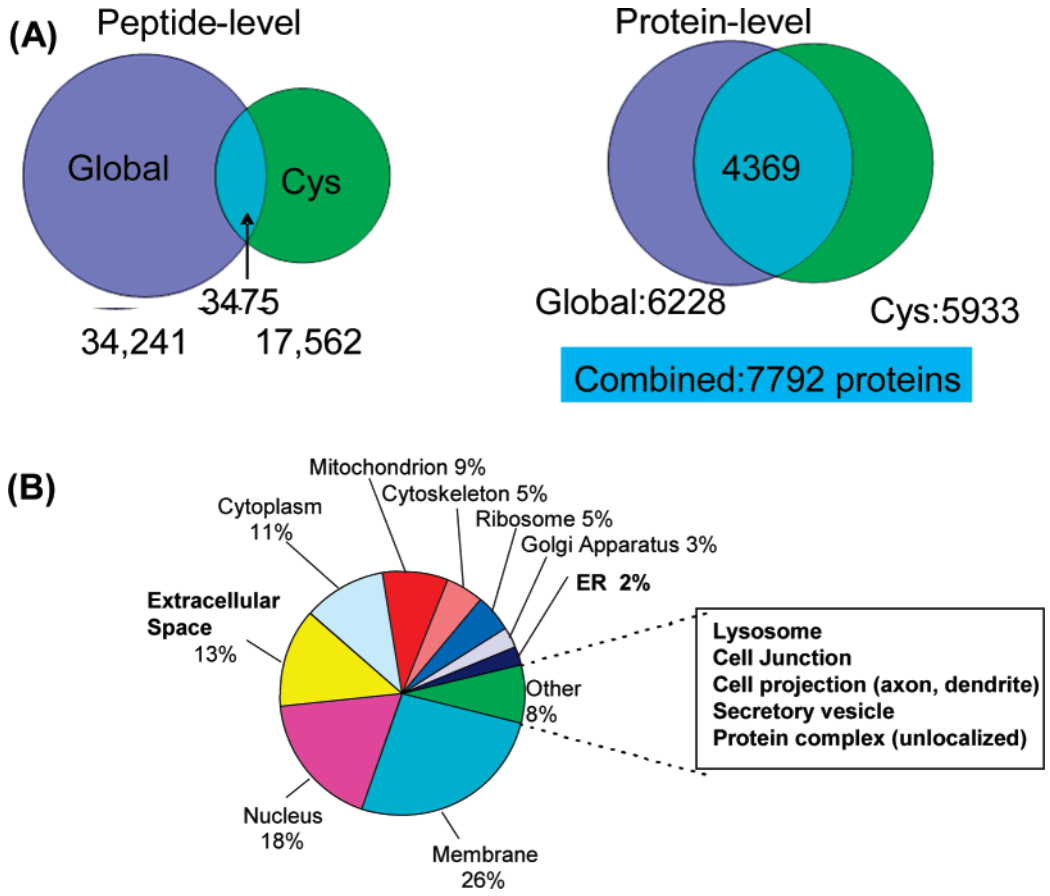

FIGURE 1: Extensive mouse brain proteome coverage from two-dimensional LC−MS/MS analyses. (A) Venn diagrams of the distribution of unique peptides and corresponding proteins identified from global and cysteine-enriched fractions from mouse brain. (B) Distribution of the 7792 unique identified mouse brain proteins based on their cellular locale. Fifty-one percent of the identified proteins were categorized on the basis of gene ontology.

with the SEQUEST search algorithm. Raw SEQUEST results were filtered using criteria previously established that provide <2% of false positive peptide identifications (*18*).

From the global digests and enriched cysteinyl-peptide fractions, 34 241 and 17 562 unique peptides were identified, respectively, covering 6228 and 5933 unique proteins, respectively (Figure 1). Global and cysteinyl-enriched peptide mixtures provide a sampling of unique proteome subsets for improved proteome and sequence coverage. The combined mixture provides 7792 confidently identified mouse brain proteins, representing 34% proteome coverage of the predicted mouse proteome. From the total set of identified proteins that have been recovered, ~26% are membrane proteins, consistent with predictions from eukaryotic genomes (*22*). From the 51% of proteins that could be categorized by gene ontology, a good representation of all cell organelles and locales is observed. Moreover, molecular masses and isoelectric points (pI) calculated for each unique protein illustrate the wide distribution of pI values (from 4.0 to 12.5) and masses (from 5 to 850 kDa) of identified brain proteins similar to those of the entire mouse proteome as previously described (*23*). Thus, the mouse brain data set presents a nearly unbiased representation of the mouse proteome.

Identification of 3-Nitrotyrosine-Modified Proteins. Many high-quality mass spectra obtained from this analysis could not be assigned to native peptides and proteins, suggesting the presence of post-translational modifications. Thus, the SEQUEST algorithm was reconfigured to search for tyrosine-containing peptides with additional masses of 44.98 Da corresponding to the addition of the NO_2 group. Because methionines are commonly converted to methionine sulfoxides in the presence of peroxynitrite, this search was widened to optimize detection of nitrated peptides by the inclusion of a search for the possible presence of an additional mass of 15.99 Da, corresponding to one oxygen, applied to methionines. The raw SEQUEST results were filtered according to the criteria described in Materials and Methods with manual inspection at the MS/MS spectrum level to ensure that major peak assignments were consistent with predicted patterns as illustrated by MS/MS spectra for the nitrated and unmodified versions of the peptide, DSYVAIANACCAPR (Figure 2). All detected y fragment ions match for the two spectra; all b ions containing the nitrotyrosine from the nitrated peptide (b_3−b_{12}) have masses that are 44.99 Da higher than those of the corresponding b ions from the non-nitrated peptide.

Thirty-six peptides were identified as highly confident nitrotyrosine identifications, corresponding to 29 unique proteins; 22 of these were derived from the cysteine-enriched fraction (Table 1). The low abundance of nitrated proteins detected in this screen, approximately 0.4%, with respect to total proteins, is consistent with the previously observed selectivity of tyrosine nitration in vivo; the average frequency of 3−4% for tyrosines in proteins provides an upper limit to any nitrotyrosine modifications (*24*). Calculated as a molar

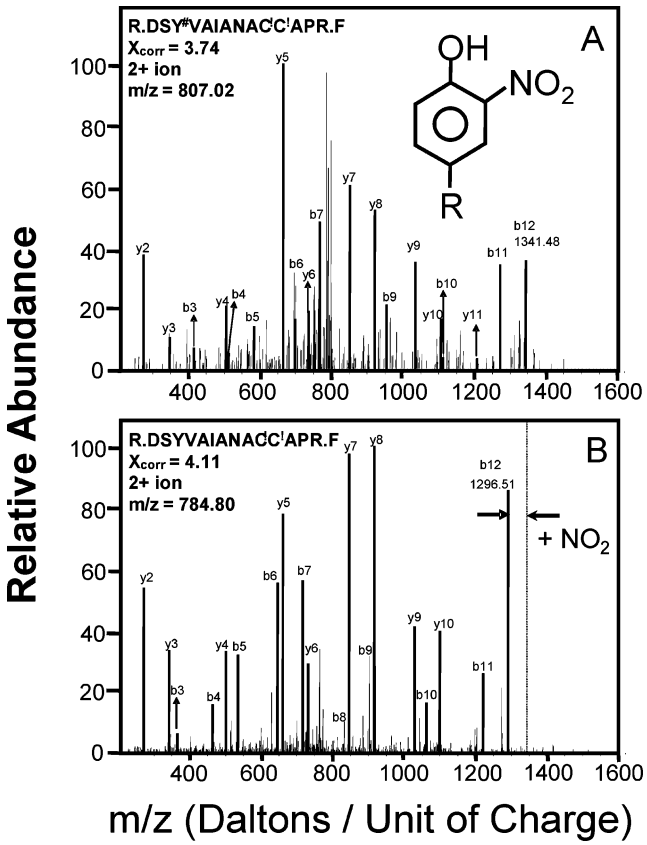

FIGURE 2: MS/MS spectra of the nitrated (A) and non-nitrated (B) peptide, DSYVAIANACCAPR, from the vesicular inhibitory amino acid transporter. Y# indicates nitrotyrosine modification, and C! indicates a cysteinyl residue modified by carbamidomethylation. The two spectra match well on all detected b and y fragment ions, with the exception of b ions containing nitrotyrosine, i.e., b_3-b_{12}, from the nitrated peptide have masses that are 44.99 Da higher than the masses of the corresponding b ions from the non-nitrated peptide.

ratio, nitrotyrosine abundance was 0.9 mol/1000 mol of tyrosine.

The nitrated peptides identified in this study vary in length from 7 to 44 amino acids and are derived from both soluble and membrane proteins. However, no membrane-spanning nitrated peptides were recovered, consistent with the low level of recovery of any transmembrane peptides by these methods. Nitrated proteins that were identified range from highly abundant proteins, (e.g., actin, tubulin, and triose phosphate isomerase) to proteins expressed at very low levels, such as receptors and nuclear transcription factors (Table 1). The extent of nitration of each protein was estimated by the ratio of the number of peptide identifications (peptide hits) of nitrated peptides to those of their unmodified analogues. Peptide hits correspond to the number of MS/MS spectra observed for each distinct peptide, which may include repetitive identification or the same peptide in one or multiple SCX fractions. These values have been demonstrated to provide a reproducible and semiquantitative measure of peptide concentration in complex samples (*21*). This approach, as opposed to using a nitrotyrosine enrichment strategy, provides a means of establishing an estimate of endogenous levels of cellular nitration as a baseline for comparison with nitration in disease states. Here, the endogenous ratios of nitrated to nonmodified peptides indicate generally low levels of nitration of the identified proteins, ranging from <1 to 50% (Table 1) (*17*, *18*). For some low-abundance peptides, only nitrated peptides were identified, which may result from incomplete sampling due to stringent criteria for identification and their low abundance.

Several proteins have been previously identified to be nitrated in vivo as indicated by asterisks in Table 1. Some of these include aldolase (in human skin fibroblasts and rat muscle), actin (in human pituitary and Alzheimer's brain), creatine kinase (in rat skeletal muscle, rat heart, and the failing human heart), triose phosphate isomerase (in Alzheimer's brain), and α-tubulin (in PC12 cells, rat brain, human gliomas and intestinal epithelium) (*5*, *25*−*31*). Examination of the cellular locale of nitrated proteins in comparison with that of the total set of 7792 proteins, identified from unmodified peptides, indicates an approximate 2- and 3-fold preference for nitration of mitochondrial and cytoskeletal proteins, respectively (Figure 3). The selective nitration of mitochondrial proteins is consistent with previous analyses by electron microscopy in brain showing nitrated proteins to be preferentially localized in the outer mitochondrial membranes and with earlier suggestions that the mitochondrion is the major cellular source of superoxide, a precursor with nitric oxide of the nitrating species, peroxynitrite (*32*−*34*). Similarly, the association of mitochondria with microtubules and actin in neurons may also put cytoskeletal proteins near sites of peroxynitrite formation (*35*).

From a functional standpoint, the striking feature of this group of nitrated proteins is that more than half of these have been previously identified to be linked with neurodegenerative diseases (Table 1). For example, many of these proteins exhibit altered levels of transcripts, protein abundances, activities, or mutations occurring in neurodegenerative disorders, including PD, the MPTP model of PD, and Alzheimer's disease (AD). The strong correlation between the endogenous nitration in nondiseased animals of proteins previously identified as being associated with neurodegenerative disease suggests a fundamental involvement of nitration in the disease process. As an example, we find nitrated paraplegin, a metalloprotease and chaperone of the inner mitochondrial membrane for which loss-of-function mutations result in the neurodegenerative disorder, hereditary spastic paraplegia (*68*). In Table 1, nitrated proteins are grouped according to categories related to the major molecular alterations associated with PD and other neurodegenerative diseases, e.g., defects in mitochondrial and energy metabolism, upregulation of stress and inflammatory pathways, cytoskeletal disorganization, and diminished dopamine synthesis. Of note, many of the nitrated proteins within several of these groups are localized in pre- and postsynaptic regions of the neuron, suggesting a potential vulnerability of neurotransmission to conditions of oxidative stress and inflammation. Consistent with the incomplete proteome (34%) and sequence coverage (≤60%) obtained in this proteomic screen, poor recovery was observed for tyrosine-containing peptides of several brain proteins previously reported to be nitrated, including the neurofilaments, glial fibrillary acidic protein (GFAP), tyrosine hydroxylase, and prostacyclin synthase [see the Supporting Information in ref *23* (*36*−*41*)].

Nitrotyrosine-Modified Brain Proteins Detected by Immunoblotting. The significant presence of nitrated proteins

Table 1: Nitrated Proteins Identified from Mouse Brain[a]

IPI no.	protein name (NCBI symbol)	nitrated peptide [NY/Y (% nitration)]	target of Tyr kinase
mitochondria, energy metabolism			
IPI00221402	*aldolase 1, A isoform (Aldoa1)[b]	R.**Y**^{174}ASICQQNGIVPIVEPEILPDGDHDLKR. [2/141 (1%)]	yes
IPI00117312	aspartate aminotransferase, mito (Got2)[c]	R.KAEAQIAAKNLDKE**Y**^{67}LPIGGLAEFCK. [1/82 (1%)]	no
IPI00128296	creatine kinase, mito (Ckmt1)[d]	G.WEFM(O)WNERLG**Y**^{274}ILTCPSNLGTGLR. [1/16 (6%)]	no
IPI00136703	*creatine kinase, B chain (Ckb)[e]	R.FCTGLTQIETLFKSKN**Y**^{269}EFMWNPHLGYILTCPSNLGTGLR. [1/64 (2%)]	no
IPI00170128	paraplegin (Spg7)[f]	K.LTQPSSF**Y**^{505}SQRLAELTPGFSGADIANICNEAALHAAR. [1/1 (50%)]	no
IPI00330903	pantothenate kinase 4 (Pank4)[g]	R.V**Y**^{320}FGGFFIR. [1/0 (100%)]	no
IPI00467833	triosephosphate isomerase 1 (Tpi1)[h]	K.IAVAAQNC**Y**^{68}K. [1/28 (3%)]	no
		R.II**Y**^{209}GGSVTGATCK. [1/69 (2%)]	no
stress and inflammation			
IPI00268250	calcineurin, catalytic subunit (Ppp3ca)[i]	R.FKEPPA**Y**^{224}GPMCDILWSDPLEDFGNEK. [1/47 (2%)]	yes
IPI00229988	eukaryotic translation initiation factor 2 (EIF2C2)[j]	M**Y**^{2}SGAGPVLASPAPTTSPIPGYAFKPPPRPDFGTTGR. [1/0 (100%)]	yes
IPI00319992	glucose-regulated protein 78 (GRP78/BIP) (Hspa5)[k]	K.ETAEA**Y**^{142}LGKKVTHAVVTVPAYFNDAQR. [1/5 (20%)]	no
IPI00132874	monoglyceride lipase, isoform 1 (Mgl1)[l]	R.**Y**^{58}DELAHMLKGLDMLVFAHDHVGHGQSEGER. [2/3 (40%)]	yes
IPI00130000	puromycin-sensitive amino-peptidase (Npepps)	K.GMNM**Y**^{465}LTKFQQKNAATEDLWESLESASGKPIAAVMNTWTK. [1/13 (7%)]	no
IPI00114615	vasoactive intestinal polypeptide receptor 2, (Vipr2)[m]	R.N**Y**^{159}IHLNLFLSFM(O)LR. [2/0 (100%)]	no
cytoskeleton			
IPI00110850	*actin, cytoplasmic (Actb)[n]	K.LC**Y**^{218}VALDFEQEMATAASSSSLEK. [7/1187 (<1%)]	yes
IPI00153990	β-centractin (Actr1b)[o]	MES**Y**^{4}DIIANQPVVIDNGSGVIK. [1/0 (100%)]	yes
IPI00331291	dynamin-1, splice isoform 2 (Dnm1)	L.RV**Y**^{125}SPHVLNLTLVDLPGMTK. [1/28 (3%)]	no
IPI00308667	T-complex associated-testis-expressed 1-like (Tcte1l)	MEG**Y**^{4}QRPCDEVGFNADEAHNIVK. [2/3 (40%)]	yes
IPI00117350	*tubulin α-4 chain (Tuba4)[p]	R.NGP**Y**^{83}RQLFHPEQLITGKEDAANNYAR. [2/38 (5%)]	no
		R.NGP**Y**^{83}RQLFHPEQLITGK. [3/38 (8%)]	no
IPI00403810	tubulin α-6 chain (Tuba6)	K.A**Y**^{282}HEQLTVAEITNACFEPANQMVK. [3/1 (75%)]	no
IPI00120923	vacuolar protein sorting 16, isoform 1 (Vps16)	MDC**Y**^{4}TANWNPLGDSAFYR. [1/0 (100%)]	yes
		M(O)DC**Y**^{4}TANWNPLGDSAFYR. [1/0 (100%)]	
dopamine synthesis			
IPI00230682	Tyr hydroxylase activation protein, (YWhab)[q]	K.KQQMGKE**Y**^{84}REKIEAELQDICNDVLELLDK. [2/30 (6%)]	no
		R.EKIEAELQDICNDVLELLDK**Y**^{106}LILNATQAESK. [2/30 (6%)]	
others			
IPI00346965	adapter-related protein complex 1 (Ap1b1)	K.PLISEETDLIEPTLLDELICYIGTLASV**Y**^{574}HK. [2/6 (25%)]	no
IPI00312527	dihydropyrimidinase-related protein-1 (Crmp1)[r]	K.AAAFVTSPPLSPDPTTPD**Y**^{316}LTSLLACGDLQVTGSGHCPYSTAQK. [1/192 (<1%)]	yes
IPI00229824	nuclear factor 1A, isoform 1 (Nfia)	M(O)**Y**^{2}SPLCLTQDEFHPFIEALLPHVR. [1/0 (100%)]	no
		M**Y**^{2}SPLCLTQDEFHPFIEALLPHVR. [1/0 (100%)]	
IPI00115588	nuclear RNA export factor 1 (Nxf1)[s]	K.ITIP**Y**^{125}GR. [1/0 (100%)]	no
IPI00124980	prolactin regulatory element-binding protein (Preb)	R.GVEL**Y**^{10}RAPFPLYALR. [1/0 (100%)]	no
IPI00132720	vesicular inhibitory amino acid transporter (Sic32a)	R.DS**Y**^{186}VAIANACCAPR. [1/13 (7%)]	yes
IPI00273613	laminin receptor 1/ribosomal protein SAP 40 (LOC226574)	A.DHRPLTEAS**Y**^{139}VNLPTIALCNTDSPLR. [2/11 (16%)]	yes
IPI00551171	SIM. probable RNA-dependent helicase P68(LOC432554)	G.HNCPKPVLKF**Y**^{97}EANFPANVM(O)DVIAR. [2/7 (22%)]	no
		G.HNCPKPVLKF**Y**^{97}EANFPANVMDVIAR. [1/7 (13%)]	

[a] Nitrotyrosine-modified proteins and their corresponding nitrated peptides were identified from C57BL/6J mouse brain (see Materials and Methods) and assigned to categories relating to their relationship to biological processes affected in Parkinson's disease. Entries with lettered footnotes indicate proteins linked with neurodegenerative disorders. References relating to the identified linkage between indicated proteins and neurodegenerative disease include the following: [b]refs *81* and *82*, [c]ref *83*, [d]refs *84*−*86*, [e]refs *58*, *87*, and *88*, [f]refs *89* and *90*, [g]ref *91*, [h]refs *28*, *59*, and *60*, [i]refs *18*, *64*, and *92*, [j]refs *93* and *94*, [k]ref *95*, [l]refs *96*−*98*, [m]refs *99* and *100*, [n]refs *70* and *71*, [o]ref *101*, [p]refs *72*, *74*, and *102*−*104*, [q]ref *66*, [r]refs *28* and *88*, and [s]ref *105*. Each protein name is preceded by its corresponding International Protein Index number (IPI no.) and followed by its NCBI gene symbol in parentheses. Periods indicate ends of peptides; for internal peptides, the amino acid preceding the cleavage site is given. Nitrotyrosines are denoted in bold font, and superscript numbers indicate their position in the primary sequence of the mature protein. M(O) represents methionine sulfoxide. An estimate of the extent of nitration [NY/Y (%)] is presented and is based on the number of observed spectra for nitrated proteins relative to the analogous unmodified peptide. Asterisks designate proteins previously observed to be sensitive to nitration. Sensitivity of sites to tyrosine kinases was determined using NetPhos 2.0 (*106*, *107*), where the average score and standard deviation for all 11 tyrosine sites identified to be a target of tyrosine kinase was 0.76 ± 0.22.

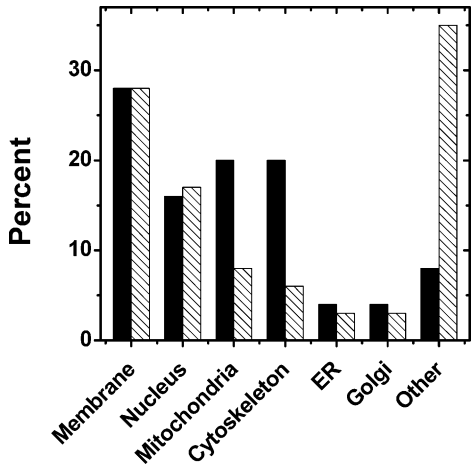

FIGURE 3: Preferential nitration of mitochondrial and cytoskeletal brain proteins. Gene ontology analysis of the cellular locale of nitrated brain proteins (black bars) compared with that of the total identified brain proteins (hatched bars). The number of proteins in each category is expressed as a percent of the total. The category "Other" represents the extracellular space, ribosomes, lysosomes, cell junction, cell projections, secretory vesicles, and cytoplasm.

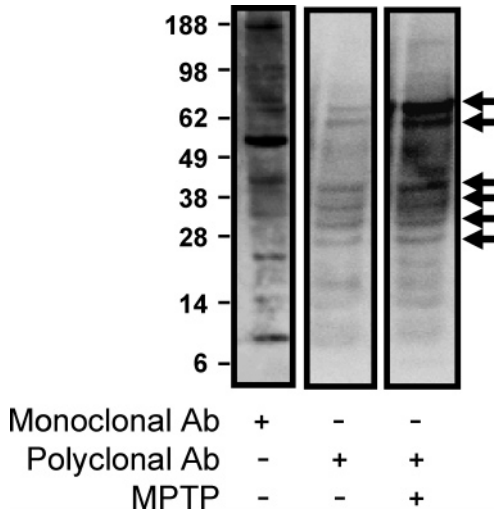

FIGURE 4: 3-Nitrotyrosine modification of brain proteins in homogenates of normal and MPTP-treated C57BL mice detected with monoclonal or polyclonal anti-nitrotyrosine antibodies as indicated below. Positions of molecular mass markers are given at the left.

was confirmed by Western immunoblots of brain homogenates using either monoclonal or polyclonal antibodies against nitrotyrosine (Figure 4). However, depending on the antibody, the pattern of nitrated proteins observed on immunoblots is very different. For example, using monoclonal antibodies, a large number of nitrated proteins are observed with a prominent band near 55 kDa. In contrast, using a polyclonal antibody, immunoblots present a lighter banding pattern of six major bands among a background of lower-density bands. Differences in the staining density of nitrated proteins observed using these two different antibodies indicate a differential sensitivity toward individual nitrated proteins within the same sample, consistent with previous observations that in muscle homogenates three different nitrotyrosine antibodies revealed three different staining patterns (*42*). Therefore, while the relative densities of different nitrated bands may not accurately reflect their relative abundance, immunoblots using a single antibody are useful for assessing relative trends in modification of specific proteins upon environmental exposure to agents associated with oxidative stress or as a result of disease.

In this respect, treatment of mice with neurotoxin MPTP results in a similar pattern of brain protein nitration, with increased staining density for the six major bands that are nitrated in untreated animals. The MPTP treatment regimen using in this study induced a 60% loss in dopamine content in the striatum 6 days post-treatment, based on HPLC analyses of striatal homogenates (80.3 ± 6.5 ng/mg of protein in lesioned animals vs 200 ± 28.0 ng/mg of protein in controls, $p < 0.0002$, 12 d.f., using the Student's *t*-test). Further, these observations are consistent with prior work demonstrating increased levels of nitration within brain tissue of MPTP-treated animals (*2*, *43*−*45*). Some of the more abundant brain proteins identified as nitrated by LC−MS/MS may also correspond to nitrated proteins detected within bands in these Western blots. For example, from monomer molecular masses of abundant proteins identified by LC−MS/MS, triose phosphate isomerase (27 kDa), aldolase (40 kDa), actin (43 kDa), calcineurin A (60 kDa), and dihydropyrimidinase-related protein (63 kDa) are possible candidates for some of the nitrated proteins detected by Western blotting (Figure 4). However, in view of the incomplete proteome coverage of the LC−MS/MS data set, positive identification of all nitrated protein bands will require additional experimental approaches. Nevertheless, the immunoblots suggest that a select population of proteins are sensitive to nitration and become more highly nitrated with neurodegeneration and are consistent with the LC−MS/MS results that endogenously nitrated proteins are comprised of a significant fraction of proteins that are adversely affected in neurodegeneration.

Selectivity for Tyrosine Nitration in Vivo. The nitrotyrosine-modified peptides identified in this proteomic screen provide an opportunity to identify common structural characteristics that promote nitration in vivo. For example, it has been suggested that tyrosine nitration is impeded by the presence of nearby cysteines or methionines as a result of their effective competition for nitrating species (*46*, *47*). On the basis of studies with model peptides, it has been suggested that the presence of a proximal cysteine residue inhibits tyrosine nitration by intramolecular electron transfer from a tyrosyl radical to cysteine across as many as four intervening amino acids (*46*). However, in the identified set of nitrated sequences, both methionines and cysteines are proximal to nitrotyrosines. At least one cysteine is found within 23 of the nitrated peptides, of 6107 Tyr-containing peptides (0.38%) from the cysteine-capture method; in comparison, there are 12 nitrated peptides without cysteines which were derived from the global fraction of 11 051 Tyr-containing peptides (0.11%). Specifically, four nitrated peptides contain cysteines that are vicinal to the nitrotyrosine. Another eight nitrated peptides contain a cysteine that is three or four amino acids from the nitrotyrosine, which would also be closely positioned in an α-helical structure. Thus, this set of nitrated sequences suggests that nearby cysteines or methionines do not prevent tyrosine nitration in vivo, consistent with previous measurements in vitro (*48*).

Comparing average Kyte−Doolittle hydrophobicity indices around nitrated sequences with those of unmodified tyrosines

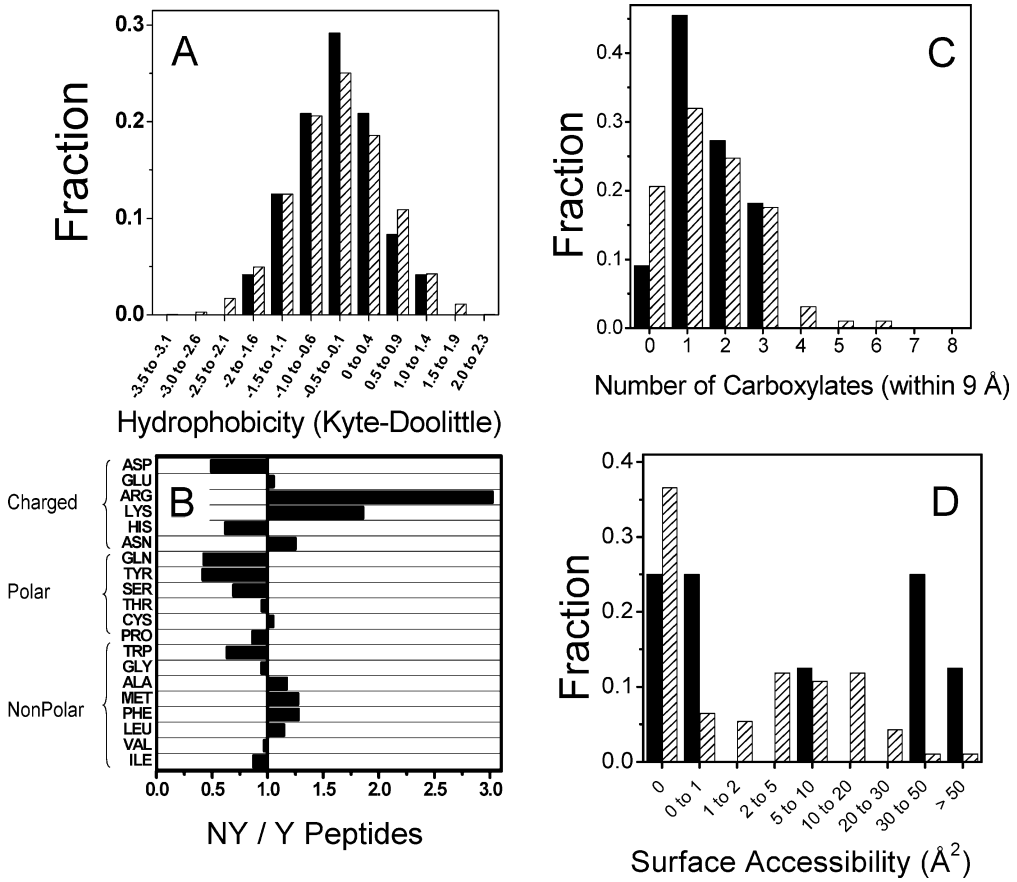

FIGURE 5: Physical properties of the protein environment around nitrated tyrosines (black bars) compared with that of other tyrosines (hatched bars) were determined for calculated hydrophobicities (A) and amino acid content within the nine-amino acid window of linear sequence around each tyrosine (B) or from available high-resolution structures, negative charge density (C), and surface accessibility (D). Hydrophobicities were calculated using a nine-amino acid window using Prot Scale based on Kyte−Doolittle hydrophobicity indices (*108*, *109*). In cases where high-resolution structures are available (see Figure 6), the number of carboxylates within 9 Å was determined by visual inspection using RasMol (*110*) and surface accessibility was calculated using Surface Racer 1.1, assuming a radius of 1.4 Å that is similar to that reported for peroxynitrite (*111*, *112*).

shows identical distributions that span the range of hydrophobicity indices, indicating that this parameter has little influence on the sensitivity of tyrosines to nitration (Figure 5A). However, the amino acid content within these sequences displays a significant preference for the presence of basic amino acids proximal to nitrated tyrosines (Figure 5B). Together, Arg and Lys account for 14% of all amino acids proximal to nitrated tyrosines, corresponding to an average of one basic amino acid per nitrated sequence. In fact, 25 of the 31 (nonredundant) nitrated brain sequences follow this correlation and include at least one basic amino acid, suggesting that the presence of a positive charge is a critical factor in tyrosine nitration (Table 1). For five other identified nitrotyrosine sites, the nearby N-terminus provides a positive charge. In contrast, acidic residues Glu and Asp, while commonly occurring near tyrosines, show no greater preference for sequences around nitrated tyrosines. Examination of three-dimensional structures available for nine of these nitrated proteins demonstrates a slight preference of nitrotyrosines for proximal carboxylates, consistent with prior suggestions that nearby negative charges can promote tyrosine nitration (*48*, *49*) (Figure 5C).

From these high-resolution structures, the surface accessibility was calculated for the ortho position of the aromatic ring of each tyrosine to peroxynitrite (~1.4 Å). This analysis shows that unmodified tyrosines most frequently occupy positions inaccessible to peroxynitrite, whereas highly accessible tyrosines (>50 Å^2) exhibit a nearly total preference for nitrotyrosine (Figure 5D). However, nitrated tyrosines are also located in regions calculated to be of low accessibility, suggesting protein dynamics could transiently increase tyrosine accessibility to peroxynitrite. Moreover, the predominant location of nitrated tyrosines on loop structures may be the basis for their solvent accessibility; eight of the nine high-resolution structures exhibit nitrotyrosine sites within loops (Figure 6). Similarly, from amino acid sequence analysis, 59% of nitrated tyrosine sites are predicted to be located in loops, 30% in helices, and 11% in β-strands, consistent with the previously observed preference of nitrotyrosines for loops relative to the infrequent occurrence of unmodified tyrosines in loops (*24*, *49*). Taken together, these analyses of brain peptides suggest that the presence of nearby basic amino acids and the increased level of solvent exposure are predictive factors for the nitration of specific tyrosines in vivo. As an example, nitro-Tyr^{224} of calcineurin (Table 1) lacks proximal basic amino acids but protrudes substantially from the surface of the protein as evidenced by its crystal structure (1AUI.pdb). Nevertheless, although no single factor seems to explain the nitration of all tyrosines, the presence of nearby positive charges is apparent for 28 of the 31 (nonredundant) nitrated tyrosines.

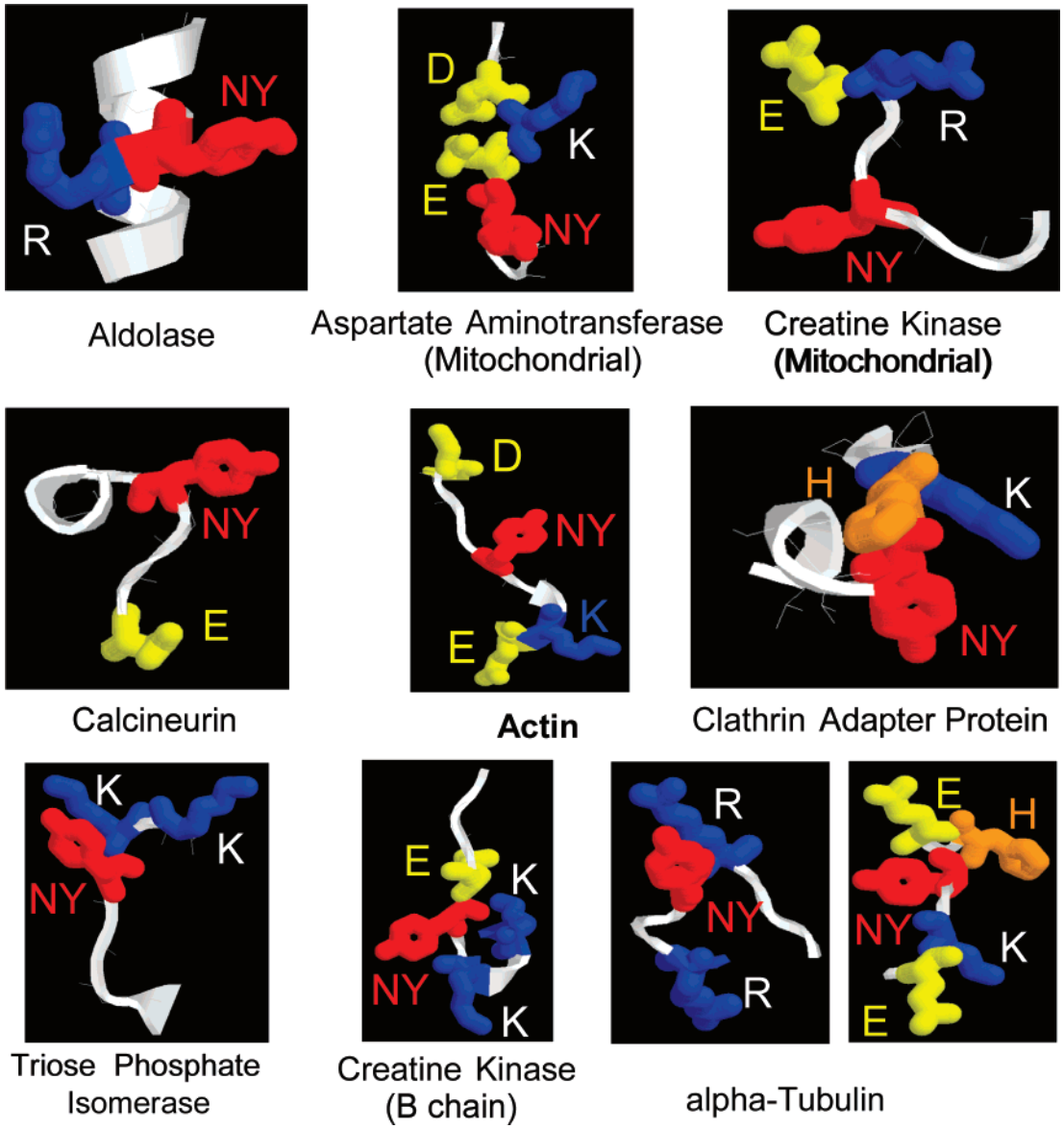

FIGURE 6: Three-dimensional structure around nitrated tyrosines (NY, red) in proteins of known structures sufficiently homologous to the mouse proteins which include aldolase (1ADO) (*113*), aspartate aminotransferase (1AMA) (*114*), β-actin (1HLU) (*115*), calcineurin (1AUI) (*116*), clathrin adaptor protein complex 1 (1W63) (*117*), creatine kinase chain B (1QH4) (*118*), mitochondrial creatine kinase (1CRK) (*119*), triose phosphate isomerase (1SQ7) (*120*), and tubulin (1TUB) (*121*). Selected neighboring amino acids within four amino acids of the primary sequence are shown, where basic amino acids (R or K) are colored blue, acidic amino acids (E or D) are colored yellow, and histidine (H) is colored orange. Protein structures were downloaded from the Protein Data Bank (*122*).

DISCUSSION

From the extensive data set generated by the LC/LC−MS/MS analysis of the whole brain proteome, 29 proteins have been identified with high confidence that are nitrated under basal conditions. The associated list of identified nitration sites is the largest currently available and permits insights regarding the nitrating species, predictive rules regarding sensitive sites, and possible involvement in neurodegenerative disease.

Previous proteomic identification of nitrated proteins has been largely limited to abundant and soluble proteins that can be detected by nitrotyrosine antibodies and for which constituent peptides can be eluted from two-dimensional gels in sufficient amounts for MS identification (*26*−*28*, *50*, *51*). In contrast, the high-resolution two-dimensional LC system coupled with MS/MS applied here has a number of advantages, including the sensitivity and dynamic range to identify both high- and low-abundance cellular peptides and proteins. Second, two-dimensional chromatographic separation of peptides, rather than whole proteins, permits identification of membrane proteins, which are typically lost during the isoelectric focusing step of two-dimensional gels due to formation of protein aggregates (*52*). Third, this approach is independent of the biases introduced through the use of antibodies for either enrichment of nitrated proteins or their detection. Furthermore, MS/MS identification of peptide sequences including the site(s) of modification provides validation that may be missing in two-dimensional gel approaches in which nitrated and non-nitrated proteins comigrate. Finally, utilizing the same complex protein mixture to identify both nitrated peptides and their non-nitrated analogues makes a semiquantitative estimate of nitrotyrosine stoichiometry possible.

Links of Nitration-Sensitive Proteins with Neurodegenerative Disease. The identification, in this study, of a set of nitrated proteins previously documented as sites of vulnerability in neurodegeneration suggests nitrotyrosine-induced protein misfolding may be a contributing factor in neurodegeneration. This hypothesis is supported by anti-nitrotyrosine immunoblots showing the increased staining density of protein bands of brain homogenates from MPTP-lesioned mice relative to untreated mice (Figure 4). Alternatively, many of these sensitive proteins may represent neutral markers of inflammation not directly involved in neurodegenerative processes. Distinction of these two hypotheses will require examination of the functional effects of nitration of these proteins.

Potential sources of nitration in neurodegeneration consist of peroxynitrite generation arising from excess superoxide generated by defects in mitochondrial metabolism, inflammation-related nitric oxide from activated glial cells, or other neural inflammatory pathways (*15*, *51*, *53*−*57*). Mitochondrial proteins and nearby cytosolic energy-metabolizing proteins, expected to be among the first targets of peroxynitrite, are well-represented in the set of nitrated proteins (Table 1). One of these, the neuronal-specific isoform of creatine kinase (BB), has been shown to exhibit inactivation as an early marker of oxidative stress in neurons and in AD, and its nitration has been detected in several proteomic screens (*26*, *27*, *58*). Another abundant metabolic enzyme, triose phosphate isomerase (TPI), is inhibited by β-carbolenes, endogenous analogues of MPTP, and found to be nitrated in AD brain tissue (*28*, *59*). Moreover, TPI mutations have been shown to cause protein misfolding, aggregates, and neurodegeneration (*60*, *61*).

Protein misfolding is a common characteristic of neurodegenerative diseases, where aggregated proteins accumulate in protein inclusion bodies such as Lewy bodies and neurofibrillary tangles (*62*). The observed nitration of two proteins critical to the unfolded protein response, i.e., the ER chaperone, glucose-regulated protein 78 (GRP78), and eukaryotic initiation factor 2 (EIF2), suggests the potential for an altered misfolded protein response. The nitration of the catalytic subunit of calcineurin suggests a wide range of possible cellular effects, including altered regulation of inflammation in astrocytes (*63*). Prior studies have documented the functional sensitivity of calcineurin to oxidative stress as well as its decreased activity and abundance in amyotrophic lateral sclerosis, AD, and aging (*64*, *65*).

Nitration Sensitivity of Dopamine Synthesis. Specific to PD is the early loss in dopamine production occurring through the decreased activity of tyrosine hydroxylase (TH), which mediates the rate-limiting step in dopamine synthesis. The TH activation protein, a 14-3-3 interaction protein, was identified in this study as a nitrated protein having multiple nitrotyrosines, i.e., Tyr^{84} and Tyr^{106} (Table 1). This protein activates TH by binding and stabilizing its Ser^{40}-phosphorylated form. TH inactivation is mediated by the phosphatase, PP2a, which, in turn, is activated by interaction with α-synuclein (*66*). The previously documented MPTP-induced nitration of both TH and α-synuclein, in combination with the endogenous nitration of the TH activation protein identified in this study, suggests a foci of sensitivity to nitration that may explain the early loss of dopamine production under chronic conditions of inflammation (*39*, *67*, *68*).

Nitration of Cytoskeletal Proteins. Cytoskeletal integrity, essential for function and survival of neurons, is disrupted in many neurodegenerative diseases (*69*). The sensitivity of multiple cytoskeletal proteins to nitration, as identified in this proteomic study, suggests one mechanism for the observed cytoskeletal disorganization, as evidenced by their important roles in neuronal function. Major components of the cytoskeleton, actin and tubulin, are among endogenously nitrated proteins and have been observed to be nitrated in amyolateral sclerosis and in differentiating PC12 cells (*70*, *71*). Altered expression of β-actin has been observed in AD and an animal model of PD, while differential alterations in α- and β-tubulin result from MPTP treatment (*72*, *73*). The importance of proper folding and assembly of α and β forms of tubulin is underscored by the finding that parkin, the gene linked to autosomal recessive juvenile PD, is an E3 ligase and associates with α/β-tubulin, thus facilitating efficient ubiquitination and degradation of misfolded tubulin (*74*).

Protein Structural Features that Enhance Nitration of Tyrosines. Previous studies have addressed the selectivity of tyrosine nitration induced by peroxynitrite using the available high-resolution structures of three soluble nitration-sensitive proteins; these studies suggested that surface exposure of the aromatic ring, the location of the tyrosine on a loop, and proximity with a nearby negative charge promote the selective nitration of specific tyrosines under in vitro conditions (*48*, *49*). The data set of 31 nitrated and 1712 unmodified tyrosine-containing peptide sequences provided by this proteomic screen, including nine available high-resolution structures (Figure 6), offers the opportunity to compare predictions made using peroxynitrite with observed sites of nitration present under in vivo conditions. Consistent with prior suggestions that peroxynitrite is a physiologically important nitrating species (*6*, *10*, *45*, *75*, *76*), we find that under in vivo conditions, surface-exposed tyrosines are selectively nitrated, with some preference for tyrosines close to acidic side chains (Figure 4C,D). However, more striking is the preference for a positive charge (Lys, Arg, or amino terminus) in the immediate vicinity within the primary sequence of nitrated tyrosines relative to that observed for tyrosines that are not nitrated (Figure 5B).

Prediction of Nitrated Sites and Physiological Implications. Inspection of previously reported sites of in vivo nitration also indicates the targeted nitration of tyrosines proximal to basic amino acids. For example, using multiple cell models, two tyrosines (i.e., K<u>I</u>NGY^{66}TGPG and Q<u>R</u>GDY^{152}DLNA) within the p65 subunit of NFκB were selectively nitrated following administration of sodium nitroprusside, a $NO^{\bullet}$ donor, that results in the inhibition of NFκB function (*77*). Likewise, eight sites of nitration in the SERCA2a isoform of the Ca-ATPase have been identified (i.e., AL<u>K</u>EY^{122}EPEM, G<u>K</u>VY^{130}<u>R</u>QDR, <u>R</u>GAIY^{294}Y^{295}F<u>K</u>IA, <u>RK</u>SMSVY^{497}CTPN, NFI<u>K</u>Y^{586}ETNL, G<u>R</u>AIY^{753}NN<u>M</u><u>K</u>, and VA<u>R</u>NY^{990}LEPG); these all include proximal basic amino acids (*8*). The extent of SERCA2a nitration at selected sites increases in an age-dependent manner and correlates with diminished transport function (*78*). Similar dependencies are apparent from prior in vitro measurements using peroxynitrite. In the case of the calcium regulatory protein calmodulin, there are two surface-exposed tyrosines. How-

ever, while Tyr^{99} within the KDGNGY^{99}ISAA sequence is almost stoichiometrically nitrated, Tyr^{138} in the GQVNY-EEFV sequence is not a target of nitration (*48*). Likewise, of 13 nitration sites in seven different proteins, the proximal location of a basic amino acid is observed in nine instances (Table 4 in ref *49*).

The strong preference for basic amino acids in the immediate vicinity of nitrated tyrosines has important implications and suggests the involvement of electrostatic attraction of nitrating anions, such as nitrosoperoxocarbonate or its related carbonate radical anion (CO_3^-), which oxidizes tyrosine to tyrosyl radical for recombination with nitrogen dioxide to produce nitrotyrosine (*79*). Thus, targeted sites for nitration may be predicted from a visual inspection of the primary sequence and, more importantly, represent a design feature that can alter the sensitivity of a protein to oxidative and nitrative stress. The persistence of a nitration site under mild conditions of oxidative stress (i.e., in a young nonstressed animal) suggests that endogenously nitrated proteins may function as sensors that detect oxidative stress to regulate cell function (*78*). Consistent with this suggestion, it is apparent that many of the nitration-sensitive tyrosines under basal conditions are targeted for additional nitration following exposure to MPTP. Furthermore, nitrotyrosine formation has been suggested to mimic phosphotyrosine side chains in promoting protein associations and signaling; for example, nitration has been suggested to modulate the activation of tyrosine kinases involving the EGF receptor to promote selected protein associations involving complex formation (*7*, *80*). Consistent with a possible relationship between tyrosine nitration and normal tyrosine kinase signaling pathways, 11 of the 31 sites of nitration involve sites that are predicted to be phosphorylated (Table 1). Moreover, from the Phospho.Elm database of experimentally verified eukaryotic protein phosphorylation sites, 69 of 825 phosphotyrosine sequences contain at least one proximal arginine or lysine, suggesting that a subset of phosphotyrosine signaling events can be modulated by nitrating conditions (*59*, *60*).

Conclusions. Both the sensitivity of the identified proteins to nitration and their importance for normal neuronal function suggest that nitrotyrosine modification should be considered as a causal factor in neurodegenerative disease. Coupled with the observation that sites of nitration are sequence-dependent and are frequently expected to be sites of phosphorylation, these results further suggest that nitration may function under normal conditions as part of an adaptive cellular response that has the potential to lead to cellular neuropathology and diminished brain function under chronic inflammatory conditions. Future studies should extend these proteomic measurements to consider the relationship between protein nitration and specific neurodegenerative diseases as well as tyrosine kinase signaling pathways.

REFERENCES

1. Shishehbor, M. H., Aviles, R. J., Brennan, M. L., Fu, X., Goormastic, M., Pearce, G. L., Gokce, N., Keaney, J. F., Jr., Penn, M. S., Sprecher, D. L., Vita, J. A., and Hazen, S. L. (2003) Association of nitrotyrosine levels with cardiovascular disease and modulation by statin therapy, *JAMA, J. Am. Med. Assoc. 289*, 1675−80.
2. Ara, J., Przedborski, S., Naini, A. B., Jackson-Lewis, V., Trifiletti, R. R., Horwitz, J., and Ischiropoulos, H. (1998) Inactivation of tyrosine hydroxylase by nitration following exposure to peroxynitrite and 1-methyl-4-phenyl-1,2,3,6-tetrahydropyridine (MPTP), *Proc. Natl. Acad. Sci. U.S.A. 95*, 7659−63.
3. Newman, D. K., Hoffman, S., Kotamraju, S., Zhao, T., Wakim, B., Kalyanaraman, B., and Newman, P. J. (2002) Nitration of PECAM-1 ITIM tyrosines abrogates phosphorylation and SHP-2 binding, *Biochem. Biophys. Res. Commun. 296*, 1171−9.
4. Di Stasi, A. M., Mallozzi, C., Macchia, G., Petrucci, T. C., and Minetti, M. (1999) Peroxynitrite induces tryosine nitration and modulates tyrosine phosphorylation of synaptic proteins, *J. Neurochem. 73*, 727−35.
5. Koeck, T., Levison, B., Hazen, S. L., Crabb, J. W., Stuehr, D. J., and Aulak, K. S. (2004) Tyrosine nitration impairs mammalian aldolase A activity, *Mol. Cell. Proteomics 3*, 548−57.
6. Li, X., De Sarno, P., Song, L., Beckman, J. S., and Jope, R. S. (1998) Peroxynitrite modulates tyrosine phosphorylation and phosphoinositide signalling in human neuroblastoma SH-SY5Y cells: Attenuated effects in human 1321N1 astrocytoma cells, *Biochem. J. 331* (Part 2), 599−606.
7. Mallozzi, C., Di Stasi, A. M., and Minetti, M. (2001) Nitrotyrosine mimics phosphotyrosine binding to the SH2 domain of the src family tyrosine kinase lyn, *FEBS Lett. 503*, 189−95.
8. Knyushko, T. V., Sharov, V. S., Williams, T. D., Schoneich, C., and Bigelow, D. J. (2005) 3-Nitrotyrosine Modification of SERCA2a in the Aging Heart: A Distinct Signature of the Cellular Redox Environment, *Biochemistry 44*, 13071−81.
9. Viner, R. I., Ferrington, D. A., Williams, T. D., Bigelow, D. J., and Schoneich, C. (1999) Protein modification during biological aging: Selective tyrosine nitration of the SERCA2a isoform of the sarcoplasmic reticulum Ca^{2+}-ATPase in skeletal muscle, *Biochem. J. 340* (Part 3), 657−69.
10. Beckman, J. S., and Koppenol, W. H. (1996) Nitric oxide, superoxide, and peroxynitrite: The good, the bad, and the ugly, *Am. J. Physiol. 271*, C1424−37.
11. Reiter, C. D., Teng, R. J., and Beckman, J. S. (2000) Superoxide reacts with nitric oxide to nitrate tyrosine at physiological pH via peroxynitrite, *J. Biol. Chem. 275*, 32460−6.
12. Tien, M., Berlett, B. S., Levine, R. L., Chock, P. B., and Stadtman, E. R. (1999) Peroxynitrite-mediated modification of proteins at physiological carbon dioxide concentration: pH dependence of carbonyl formation, tyrosine nitration, and methionine oxidation, *Proc. Natl. Acad. Sci. U.S.A. 96*, 7809−14.
13. Kooy, N. W., Lewis, S. J., Royall, J. A., Ye, Y. Z., Kelly, D. R., and Beckman, J. S. (1997) Extensive tyrosine nitration in human myocardial inflammation: Evidence for the presence of peroxynitrite, *Crit. Care Med. 25*, 812−9.
14. Brennan, M. L., Wu, W., Fu, X., Shen, Z., Song, W., Frost, H., Vadseth, C., Narine, L., Lenkiewicz, E., Borchers, M. T., Lusis, A. J., Lee, J. J., Lee, N. A., Abu-Soud, H. M., Ischiropoulos, H., and Hazen, S. L. (2002) A tale of two controversies: Defining both the role of peroxidases in nitrotyrosine formation in vivo using eosinophil peroxidase and myeloperoxidase-deficient mice, and the nature of peroxidase-generated reactive nitrogen species, *J. Biol. Chem. 277*, 17415−27.
15. Koeck, T., Fu, X., Hazen, S. L., Crabb, J. W., Stuehr, D. J., and Aulak, K. S. (2004) Rapid and selective oxygen-regulated protein tyrosine denitration and nitration in mitochondria, *J. Biol. Chem. 279*, 27257−62.
16. Adachi, T., Weisbrod, R. M., Pimentel, D. R., Ying, J., Sharov, V. S., Schoneich, C., and Cohen, R. A. (2004) S-Glutathiolation by peroxynitrite activates SERCA during arterial relaxation by nitric oxide, *Nat. Med. 10*, 1200−7.
17. Liu, T., Qian, W. J., Chen, W. N., Jacobs, J. M., Moore, R. J., Anderson, D. J., Gritsenko, M. A., Monroe, M. E., Thrall, B. D., Camp, D. G., II, and Smith, R. D. (2005) Improved proteome coverage by using high efficiency cysteinyl peptide enrichment: The human mammary epithelial cell proteome, *Proteomics 5*, 1263−73.
18. Qian, W. J., Liu, T., Monroe, M. E., Strittmatter, E. F., Jacobs, J. M., Kangas, L. J., Petritis, K., Camp, D. G., II, and Smith, R. D. (2005) Probability-based evaluation of peptide and protein identifications from tandem mass spectrometry and SEQUEST analysis: The human proteome, *J. Proteome Res. 4*, 53−62.
19. Nesvizhskii, A. I., Keller, A., Kolker, E., and Aebersold, R. (2003) A statistical model for identifying proteins by tandem mass spectrometry, *Anal. Chem. 75*, 4646−58.
20. Al-Shahrour, F., Diaz-Uriarte, R., and Dopazo, J. (2004) FatiGO: A web tool for finding significant associations of Gene Ontology terms with groups of genes, *Bioinformatics 20*, 578−80.

21. Qian, W. J., Jacobs, J. M., Camp, D. G., II, Monroe, M. E., Moore, R. J., Gritsenko, M. A., Calvano, S. E., Lowry, S. F., Xiao, W., Moldawer, L. L., Davis, R. W., Tompkins, R. G., and Smith, R. D. (2005) Comparative proteome analyses of human plasma following in vivo lipopolysaccharide administration using multidimensional separations coupled with tandem mass spectrometry, *Proteomics 5*, 572−84.
22. Krogh, A., Larsson, B., von Heijne, G., and Sonnhammer, E. L. (2001) Predicting transmembrane protein topology with a hidden Markov model: Application to complete genomes, *J. Mol. Biol. 305*, 567−80.
23. Wang, H., Qian, W. J., Chin, M. H., Petyuk, V. A., Barry, R. C., Liu, T., Gritsenko, M. A., Mottaz, H. M., Moore, R. J., Camp, D. G., II, Khan, A. H., Smith, D. J., and Smith, R. D. (2006) Characterization of the mouse brain proteome using global proteomic analysis complemented with cysteinyl-peptide enrichment, *J. Proteome Res. 5*, 361−9.
24. Ischiropoulos, H. (2003) Biological selectivity and functional aspects of protein tyrosine nitration, *Biochem. Biophys. Res. Commun. 305*, 776−83.
25. Zhan, X., and Desiderio, D. M. (2004) The human pituitary nitroproteome: Detection of nitrotyrosyl-proteins with two-dimensional Western blotting, and amino acid sequence determination with mass spectrometry, *Biochem. Biophys. Res. Commun. 325*, 1180−6.
26. Kanski, J., Hong, S. J., and Schoneich, C. (2005) Proteomic analysis of protein nitration in aging skeletal muscle and identification of nitrotyrosine-containing sequences in vivo by nanoelectrospray ionization tandem mass spectrometry, *J. Biol. Chem. 280*, 24261−6.
27. Kanski, J., Behring, A., Pelling, J., and Schoneich, C. (2005) Proteomic identification of 3-nitrotyrosine-containing rat cardiac proteins: Effects of biological aging, *Am. J. Physiol. 288*, H371−81.
28. Castegna, A., Thongboonkerd, V., Klein, J. B., Lynn, B., Markesbery, W. R., and Butterfield, D. A. (2003) Proteomic identification of nitrated proteins in Alzheimer's disease brain, *J. Neurochem. 85*, 1394−401.
29. Mihm, M. J., Coyle, C. M., Schanbacher, B. L., Weinstein, D. M., and Bauer, J. A. (2001) Peroxynitrite induced nitration and inactivation of myofibrillar creatine kinase in experimental heart failure, *Cardiovasc. Res. 49*, 798−807.
30. Fiore, G., Cristo, C. D., Monti, G., Amoresano, A., Columbano, L., Pucci, P., Cioffi, F. A., Cosmo, A. D., Palumbo, A., and d'Ischia, M. (2006) Tubulin nitration in human gliomas, *Neurosci. Lett. 394*, 57−62.
31. Banan, A., Zhang, L. J., Shaikh, M., Fields, J. Z., Farhadi, A., and Keshavarzian, A. (2004) Novel effect of NF-κB activation: Carbonylation and nitration injury to cytoskeleton and disruption of monolayer barrier in intestinal epithelium, *Am. J. Physiol. 287*, C1139−51.
32. Bolan, E. A., Gracy, K. N., Chan, J., Trifiletti, R. R., and Pickel, V. M. (2000) Ultrastructural localization of nitrotyrosine within the caudate-putamen nucleus and the globus pallidus of normal rat brain, *J. Neurosci. 20*, 4798−808.
33. Han, D., Antunes, F., Canali, R., Rettori, D., and Cadenas, E. (2003) Voltage-dependent anion channels control the release of the superoxide anion from mitochondria to cytosol, *J. Biol. Chem. 278*, 5557−63.
34. Cadenas, E. (2004) Mitochondrial free radical production and cell signaling, *Mol. Aspects Med. 25*, 17−26.
35. Wagner, O. I., Lifshitz, J., Janmey, P. A., Linden, M., McIntosh, T. K., and Leterrier, J. F. (2003) Mechanisms of mitochondria-neurofilament interactions, *J. Neurosci. 23*, 9046−58.
36. Anantharaman, M., Tangpong, J., Keller, J. N., Murphy, M. P., Markesbery, W. R., Kiningham, K. K., and St Clair, D. K. (2006) β-Amyloid Mediated Nitration of Manganese Superoxide Dismutase: Implication for Oxidative Stress in a APPNLh/NLh × PS-1P264L/P264L Double Knock-In Mouse Model of Alzheimer's Disease, *Am. J. Pathol. 168*, 1608−18.
37. Mehl, M., Bidmon, H. J., Hilbig, H., Zilles, K., Dringen, R., and Ullrich, V. (1999) Prostacyclin synthase is localized in rat, bovine and human neuronal brain cells, *Neurosci. Lett. 271*, 187−90.
38. Zou, M., Martin, C., and Ullrich, V. (1997) Tyrosine nitration as a mechanism of selective inactivation of prostacyclin synthase by peroxynitrite, *Biol. Chem. 378*, 707−13.
39. Yamin, G., Uversky, V. N., and Fink, A. L. (2003) Nitration inhibits fibrillation of human α-synuclein in vitro by formation of soluble oligomers, *FEBS Lett. 542*, 147−52.
40. Duda, J. E., Giasson, B. I., Chen, Q., Gur, T. L., Hurtig, H. I., Stern, M. B., Gollomp, S. M., Ischiropoulos, H., Lee, V. M., and Trojanowski, J. Q. (2000) Widespread nitration of pathological inclusions in neurodegenerative synucleinopathies, *Am. J. Pathol. 157*, 1439−45.
41. He, K., Nukada, H., McMorran, P. D., and Murphy, M. P. (1999) Protein carbonyl formation and tyrosine nitration as markers of oxidative damage during ischaemia-reperfusion injury to rat sciatic nerve, *Neuroscience 94*, 909−16.
42. Barreiro, E., Comtois, A. S., Gea, J., Laubach, V. E., and Hussain, S. N. (2002) Protein tyrosine nitration in the ventilatory muscles: Role of nitric oxide synthases, *Am. J. Respir. Cell Mol. Biol. 26*, 438−46.
43. Bloem, B. R., Irwin, I., Buruma, O. J., Haan, J., Roos, R. A., Tetrud, J. W., and Langston, J. W. (1990) The MPTP model: Versatile contributions to the treatment of idiopathic Parkinson's disease, *J. Neurol. Sci. 97*, 273−93.
44. Pennathur, S., Jackson-Lewis, V., Przedborski, S., and Heinecke, J. W. (1999) Mass spectrometric quantification of 3-nitrotyrosine, ortho-tyrosine, and o,o′-dityrosine in brain tissue of 1-methyl-4-phenyl-1,2,3,6-tetrahydropyridine-treated mice, a model of oxidative stress in Parkinson's disease, *J. Biol. Chem. 274*, 34621−8.
45. Smith, M. A., Richey Harris, P. L., Sayre, L. M., Beckman, J. S., and Perry, G. (1997) Widespread peroxynitrite-mediated damage in Alzheimer's disease, *J. Neurosci. 17*, 2653−7.
46. Zhang, H., Xu, Y., Joseph, J., and Kalyanaraman, B. (2005) Intramolecular electron transfer between tyrosyl radical and cysteine residue inhibits tyrosine nitration and induces thiyl radical formation in model peptides treated with myeloperoxidase, H_2O_2, and NO^{2-}: EPR SPIN trapping studies, *J. Biol. Chem. 280*, 40684−98.
47. Ischiropoulos, H. (1998) Biological tyrosine nitration: A pathophysiological function of nitric oxide and reactive oxygen species, *Arch. Biochem. Biophys. 356*, 1−11.
48. Smallwood, H. S., Galeva, N. A., Bartlett, R. K., Urbauer, R. J., Williams, T. D., Urbauer, J. L., and Squier, T. C. (2003) Selective nitration of Tyr99 in calmodulin as a marker of cellular conditions of oxidative stress, *Chem. Res. Toxicol. 16*, 95−102.
49. Souza, J. M., Daikhin, E., Yudkoff, M., Raman, C. S., and Ischiropoulos, H. (1999) Factors determining the selectivity of protein tyrosine nitration, *Arch. Biochem. Biophys. 371*, 169−78.
50. Aulak, K. S., Miyagi, M., Yan, L., West, K. A., Massillon, D., Crabb, J. W., and Stuehr, D. J. (2001) Proteomic method identifies proteins nitrated in vivo during inflammatory challenge, *Proc. Natl. Acad. Sci. U.S.A. 98*, 12056−61.
51. Turko, I. V., Li, L., Aulak, K. S., Stuehr, D. J., Chang, J. Y., and Murad, F. (2003) Protein tyrosine nitration in the mitochondria from diabetic mouse heart. Implications to dysfunctional mitochondria in diabetes, *J. Biol. Chem. 278*, 33972−7.
52. Wu, C. C., and Yates, J. R., III (2003) The application of mass spectrometry to membrane proteomics, *Nat. Biotechnol. 21*, 262−7.
53. Brown, M. D., Trounce, I. A., Jun, A. S., Allen, J. C., and Wallace, D. C. (2000) Functional analysis of lymphoblast and cybrid mitochondria containing the 3460, 11778, or 14484 Leber's hereditary optic neuropathy mitochondrial DNA mutation, *J. Biol. Chem. 275*, 39831−6.
54. Schriner, S. E., Linford, N. J., Martin, G. M., Treuting, P., Ogburn, C. E., Emond, M., Coskun, P. E., Ladiges, W., Wolf, N., Van Remmen, H., Wallace, D. C., and Rabinovitch, P. S. (2005) Extension of murine life span by overexpression of catalase targeted to mitochondria, *Science 308*, 1909−11.
55. Ghafourifar, P., and Colton, C. A. (2003) Compartmentalized nitrosation and nitration in mitochondria, *Antioxid. Redox Signaling 5*, 349−54.
56. Koeck, T., Stuehr, D. J., and Aulak, K. S. (2005) Mitochondria and regulated tyrosine nitration, *Biochem. Soc. Trans. 33*, 1399−403.
57. Yamamoto, T., Maruyama, W., Kato, Y., Yi, H., Shamoto-Nagai, M., Tanaka, M., Sato, Y., and Naoi, M. (2002) Selective nitration of mitochondrial complex I by peroxynitrite: Involvement in mitochondria dysfunction and cell death of dopaminergic SH-SY5Y cells, *J. Neural. Transm. 109*, 1−13.
58. Aksenova, M. V., Aksenov, M. Y., Payne, R. M., Trojanowski, J. Q., Schmidt, M. L., Carney, J. M., Butterfield, D. A., and Markesbery, W. R. (1999) Oxidation of cytosolic proteins and

expression of creatine kinase BB in frontal lobe in different neurodegenerative disorders, *Dementia Geriatr. Cognit. Disord. 10*, 158−65.
59. Bonnet, R., Pavlovic, S., Lehmann, J., and Rommelspacher, H. (2004) The strong inhibition of triosephosphate isomerase by the natural β-carbolines may explain their neurotoxic actions, *Neuroscience 127*, 443−53.
60. Olah, J., Orosz, F., Keseru, G. M., Kovari, Z., Kovacs, J., Hollan, S., and Ovadi, J. (2002) Triosephosphate isomerase deficiency: A neurodegenerative misfolding disease, *Biochem. Soc. Trans. 30*, 30−8.
61. Olah, J., Orosz, F., Puskas, L. G., Hackler, L., Jr., Horanyi, M., Polgar, L., Hollan, S., and Ovadi, J. (2005) Triosephosphate isomerase deficiency: Consequences of an inherited mutation at mRNA, protein and metabolic levels, *Biochem. J.* (in press).
62. Meriin, A. B., and Sherman, M. Y. (2005) Role of molecular chaperones in neurodegenerative disorders, *Int. J. Hyperthermia 21*, 403−19.
63. Norris, C. M., Kadish, I., Blalock, E. M., Chen, K. C., Thibault, V., Porter, N. M., Landfield, P. W., and Kraner, S. D. (2005) Calcineurin triggers reactive/inflammatory processes in astrocytes and is upregulated in aging and Alzheimer's models, *J. Neurosci. 25*, 4649−58.
64. Agbas, A., Zaidi, A., and Michaelis, E. K. (2005) Decreased activity and increased aggregation of brain calcineurin during aging, *Brain Res. 1059*, 59−71.
65. Ferri, A., Nencini, M., Battistini, S., Giannini, F., Siciliano, G., Casali, C., Damiano, M. G., Ceroni, M., Chio, A., Rotilio, G., and Carri, M. T. (2004) Activity of protein phosphatase calcineurin is decreased in sporadic and familial amyotrophic lateral sclerosispatients, *J. Neurochem. 90*, 1237−42.
66. Peng, X. M., Tehranian, R., Dietrich, P., Stefanis, L., and Perez, R. G. (2005) α-Synuclein activation of protein phosphatase 2A reduces tyrosine hydroxylase phosphorylation in dopaminergic cells, *J. Cell Sci. 118*, 3523−30.
67. Uversky, V. N., Yamin, G., Munishkina, L. A., Karymov, M. A., Millett, I. S., Doniach, S., Lyubchenko, Y. L., and Fink, A. L. (2005) Effects of nitration on the structure and aggregation of α-synuclein, *Brain Res. Mol. Brain Res. 134*, 84−102.
68. Przedborski, S., Chen, Q., Vila, M., Giasson, B. I., Djaldatti, R., Vukosavic, S., Souza, J. M., Jackson-Lewis, V., Lee, V. M., and Ischiropoulos, H. (2001) Oxidative post-translational modifications of α-synuclein in the 1-methyl-4-phenyl-1,2,3,6-tetrahydropyridine (MPTP) mouse model of Parkinson's disease, *J. Neurochem. 76*, 637−40.
69. Brandt, R. (2001) Cytoskeletal mechanisms of neuronal degeneration, *Cell Tissue Res. 305*, 255−65.
70. Tedeschi, G., Cappelletti, G., Negri, A., Pagliato, L., Maggioni, M. G., Maci, R., and Ronchi, S. (2005) Characterization of nitroproteome in neuron-like PC12 cells differentiated with nerve growth factor: Identification of two nitration sites in α-tubulin, *Proteomics 5*, 2422−32.
71. Casoni, F., Basso, M., Massignan, T., Gianazza, E., Cheroni, C., Salmona, M., Bendotti, C., and Bonetto, V. (2005) Protein nitration in a mouse model of familial amyotrophic lateral sclerosis: Possible multifunctional role in the pathogenesis, *J. Biol. Chem. 280*, 16295−304.
72. Cappelletti, G., Incani, C., and Maci, R. (1995) Involvement of tubulin in MPP^+ neurotoxicity on NGF-differentiated PC12 cells, *Cell Biol. Int. 19*, 687−93.
73. De Iuliis, A., Grigoletto, J., Recchia, A., Giusti, P., and Arslan, P. (2005) A proteomic approach in the study of an animal model of Parkinson's disease, *Clin. Chim. Acta 357*, 202−9.
74. Ren, Y., Zhao, J., and Feng, J. (2003) Parkin binds to α/β tubulin and increases their ubiquitination and degradation, *J. Neurosci. 23*, 3316−24.
75. Beckman, J. S. (2002) Protein tyrosine nitration and peroxynitrite, *FASEB J. 16*, 1144.
76. Go, Y. M., Patel, R. P., Maland, M. C., Park, H., Beckman, J. S., Darley-Usmar, V. M., and Jo, H. (1999) Evidence for peroxynitrite as a signaling molecule in flow-dependent activation of c-Jun NH_2-terminal kinase, *Am. J. Physiol. 277*, H1647−53.
77. Park, S. W., Huq, M. D., Hu, X., and Wei, L. N. (2005) Tyrosine nitration on p65: A novel mechanism to rapidly inactivate nuclear factor-κB, *Mol. Cell. Proteomics 4*, 300−9.
78. Bigelow, D. J., and Squier, T. C. (2005) Redox modulation of cellular signaling and metabolism through reversible oxidation of methionine sensors in calcium regulatory proteins, *Biochim. Biophys. Acta 1703*, 121−34.
79. Santos, C. X., Bonini, M. G., and Augusto, O. (2000) Role of the carbonate radical anion in tyrosine nitration and hydroxylation by peroxynitrite, *Arch. Biochem. Biophys. 377*, 146−52.
80. Zhang, Z., Oliver, P., Lancaster, J. J., Schwarzenberger, P. O., Joshi, M. S., Cork, J., and Kolls, J. K. (2001) Reactive oxygen species mediate tumor necrosis factor α-converting, enzyme-dependent ectodomain shedding induced by phorbol myristate acetate, *FASEB J. 15*, 303−5.
81. Kingsbury, A. E., Cooper, M., Schapira, A. H., and Foster, O. J. (2001) Metabolic enzyme expression in dopaminergic neurons in Parkinson's disease: An in situ hybridization study, *Ann. Neurol. 50*, 142−9.
82. Kim, T. D., Paik, S. R., Yang, C. H., and Kim, J. (2000) Structural changes in α-synuclein affect its chaperone-like activity in vitro, *Protein Sci. 9*, 2489−96.
83. Riemenschneider, M., Buch, K., Schmolke, M., Kurz, A., and Guder, W. G. (1997) Diagnosis of Alzheimer's disease with cerebrospinal fluid tau protein and aspartate aminotransferase, *Lancet 350*, 784.
84. Perluigi, M., Poon, H. F., Maragos, W., Pierce, W. M., Klein, J. B., Calabrese, V., Cini, C., De Marco, C., and Butterfield, D. A. (2005) Proteomic analysis of protein expression and oxidative modification in R6/2 transgenic mice: A model of Huntington's disease, *Mol. Cell. Proteomics 4*, 1849−61.
85. Dolder, M., Walzel, B., Speer, O., Schlattner, U., and Wallimann, T. (2003) Inhibition of the mitochondrial permeability transition by creatine kinase substrates. Requirement for microcompartmentation, *J. Biol. Chem. 278*, 17760−6.
86. Andres, R. H., Huber, A. W., Schlattner, U., Perez-Bouza, A., Krebs, S. H., Seiler, R. W., Wallimann, T., and Widmer, H. R. (2005) Effects of creatine treatment on the survival of dopaminergic neurons in cultured fetal ventral mesencephalic tissue, *Neuroscience 133*, 701−13.
87. Klivenyi, P., Ferrante, R. J., Matthews, R. T., Bogdanov, M. B., Klein, A. M., Andreassen, O. A., Mueller, G., Wermer, M., Kaddurah-Daouk, R., and Beal, M. F. (1999) Neuroprotective effects of creatine in a transgenic animal model of amyotrophic lateral sclerosis, *Nat. Med. 5*, 347−50.
88. Matthews, R. T., Ferrante, R. J., Klivenyi, P., Yang, L., Klein, A. M., Mueller, G., Kaddurah-Daouk, R., and Beal, M. F. (1999) Creatine and cyclocreatine attenuate MPTP neurotoxicity, *Exp. Neurol. 157*, 142−9.
89. Gelbard, H. A. (2004) Synapses and Sisyphus: Life without paraplegin, *J. Clin. Invest. 113*, 185−7.
90. Lindholm, D., Eriksson, O., and Korhonen, L. (2004) Mitochondrial proteins in neuronal degeneration, *Biochem. Biophys. Res. Commun. 321*, 753−8.
91. Zhou, B., Westaway, S. K., Levinson, B., Johnson, M. A., Gitschier, J., and Hayflick, S. J. (2001) A novel pantothenate kinase gene (PANK2) is defective in Hallervorden-Spatz syndrome, *Nat. Genet. 28*, 345−9.
92. Hata, R., Masumura, M., Akatsu, H., Li, F., Fujita, H., Nagai, Y., Yamamoto, T., Okada, H., Kosaka, K., Sakanaka, M., and Sawada, T. (2001) Up-regulation of calcineurin Aβ mRNA in the Alzheimer's disease brain: Assessment by cDNA microarray, *Biochem. Biophys. Res. Commun. 284*, 310−6.
93. Chang, R. C., Wong, A. K., Ng, H. K., and Hugon, J. (2002) Phosphorylation of eukaryotic initiation factor-2α (eIF2α) is associated with neuronal degeneration in Alzheimer's disease, *NeuroReport 13*, 2429−32.
94. Tan, S., Somia, N., Maher, P., and Schubert, D. (2001) Regulation of antioxidant metabolism by translation initiation factor 2α, *J. Cell Biol. 152*, 997−1006.
95. Holtz, W. A., and O'Malley, K. L. (2003) Parkinsonian mimetics induce aspects of unfolded protein response in death of dopaminergic neurons, *J. Biol. Chem. 278*, 19367−77.
96. Dinh, T. P., Carpenter, D., Leslie, F. M., Freund, T. F., Katona, I., Sensi, S. L., Kathuria, S., and Piomelli, D. (2002) Brain monoglyceride lipase participating in endocannabinoid inactivation, *Proc. Natl. Acad. Sci. U.S.A. 99*, 10819−24.
97. Hohmann, A. G., Suplita, R. L., Bolton, N. M., Neely, M. H., Fegley, D., Mangieri, R., Krey, J. F., Walker, J. M., Holmes, P. V., Crystal, J. D., Duranti, A., Tontini, A., Mor, M., Tarzia, G., and Piomelli, D. (2005) An endocannabinoid mechanism for stress-induced analgesia, *Nature 435*, 1108−12.
98. van der Stelt, M., Fox, S. H., Hill, M., Crossman, A. R., Petrosino, S., Di Marzo, V., and Brotchie, J. M. (2005) A role for endocannabinoids in the generation of parkinsonism and levodopa-

induced dyskinesia in MPTP-lesioned non-human primate models of Parkinson's disease, *FASEB J. 19*, 1140−2.
99. Delgado, M., and Ganea, D. (2003) Vasoactive intestinal peptide prevents activated microglia-induced neurodegeneration under inflammatory conditions: Potential therapeutic role in brain trauma, *FASEB J. 17*, 1922−4.
100. Hald, A., and Lotharius, J. (2005) Oxidative stress and inflammation in Parkinson's disease: Is there a causal link? *Exp. Neurol. 193*, 279−90.
101. Cuadrado-Tejedor, M., Sesma, M. T., Gimenez-Amaya, J. M., and Ortiz, L. (2005) Changes in cytoskeletal gene expression linked to MPTP-treatment in Mice, *Neurobiol. Dis*. (in press).
102. Boutte, A. M., Neely, M. D., Bird, T. D., Montine, K. S., and Montine, T. J. (2005) Diminished taxol/GTP-stimulated tubulin polymerization in diseased region of brain from patients with late-onset or inherited Alzheimer's disease or frontotemporal dementia with parkinsonism linked to chromosome-17 but not individuals with mild cognitive impairment, *J. Alzheimer's Dis. 8*, 1−6.
103. Chande, M. (2003) Defects in tubulin assembly machinery underlie disease, *Lancet Oncol. 4*, 67.
104. Suwelack, D., Hurtado-Lorenzo, A., Millan, E., Gonzalez-Nicolini, V., Wawrowsky, K., Lowenstein, P. R., and Castro, M. G. (2004) Neuronal expression of the transcription factor Gli1 using the Tα1 α-tubulin promoter is neuroprotective in an experimental model of Parkinson's disease, *Gene Ther. 11*, 1742−52.
105. Irwin, S., Vandelft, M., Pinchev, D., Howell, J. L., Graczyk, J., Orr, H. T., and Truant, R. (2005) RNA association and nucleocytoplasmic shuttling by ataxin-1, *J. Cell Sci. 118*, 233−42.
106. Blom, N., Gammeltoft, S., and Brunak, S. (1999) Sequence and structure-based prediction of eukaryotic protein phosphorylation sites, *J. Mol. Biol. 294*, 1351−62.
107. Kreegipuu, A., Blom, N., and Brunak, S. (1999) PhosphoBase, a database of phosphorylation sites: Release 2.0, *Nucleic Acids Res. 27*, 237−9.
108. Gasteiger, E., Hoogland, C., Gattiker, A., Duvaud, S., Wilkins, M. R., Appel, R. D., and Bairoch, A. (2005) *Protein Identification and Analysis Tools on ExPASy Server*, Humana Press, Totowa, NJ.
109. Kyte, J., and Doolittle, R. F. (1982) A simple method for displaying the hydropathic character of a protein, *J. Mol. Biol. 157*, 105−32.
110. Sayle, R. A., and Milner-White, E. J. (1995) RASMOL: Biomolecular graphics for all, *Trends Biochem. Sci. 20*, 374.
111. Tsodikov, O. V., Record, M. T., Jr., and Sergeev, Y. V. (2002) Novel computer program for fast exact calculation of accessible and molecular surface areas and average surface curvature, *J. Comput. Chem. 23*, 600−9.
112. Worle, M., Latal, P., Kissner, R., Nesper, R., and Koppenol, W. H. (1999) Conformation of peroxynitrite: Determination by crystallographic analysis, *Chem. Res. Toxicol. 12*, 305−7.
113. Blom, N., and Sygusch, J. (1997) Product binding and role of the C-terminal region in class I D-fructose 1,6-bisphosphate aldolase, *Nat. Struct. Biol. 4*, 36−9.
114. McPhalen, C. A., Vincent, M. G., Picot, D., Jansonius, J. N., Lesk, A. M., and Chothia, C. (1992) Domain closure in mitochondrial aspartate aminotransferase, *J. Mol. Biol. 227*, 197−213.
115. Chik, J. K., Lindberg, U., and Schutt, C. E. (1996) The structure of an open state of β-actin at 2.65 Å resolution, *J. Mol. Biol. 263*, 607−23.
116. Kissinger, C. R., Parge, H. E., Knighton, D. R., Lewis, C. T., Pelletier, L. A., Tempczyk, A., Kalish, V. J., Tucker, K. D., Showalter, R. E., Moomaw, E. W., et al. (1995) Crystal structures of human calcineurin and the human FKBP12-FK506-calcineurin complex, *Nature 378*, 641−4.
117. Heldwein, E. E., Macia, E., Wang, J., Yin, H. L., Kirchhausen, T., and Harrison, S. C. (2004) Crystal structure of the clathrin adaptor protein 1 core, *Proc. Natl. Acad. Sci. U.S.A. 101*, 14108−13.
118. Eder, M., Schlattner, U., Becker, A., Wallimann, T., Kabsch, W., and Fritz-Wolf, K. (1999) Crystal structure of brain-type creatine kinase at 1.41 Å resolution, *Protein Sci. 8*, 2258−69.
119. Fritz-Wolf, K., Schnyder, T., Wallimann, T., and Kabsch, W. (1996) Structure of mitochondrial creatine kinase, *Nature 381*, 341−5.
120. Kursula, I., Salin, M., Sun, J., Norledge, B. V., Haapalainen, A. M., Sampson, N. S., and Wierenga, R. K. (2004) Understanding protein lids: Structural analysis of active hinge mutants in triosephosphate isomerase, *Protein Eng., Des. Sel. 17*, 375−82.
121. Nogales, E., Wolf, S. G., and Downing, K. H. (1998) Structure of the αβ tubulin dimer by electron crystallography, *Nature 391*, 199−203.
122. Bernstein, F. C., Koetzle, T. F., Williams, G. J., Meyer, E. F., Jr., Brice, M. D., Rodgers, J. R., Kennard, O., Shimanouchi, T., and Tasumi, M. (1977) The Protein Data Bank. A computer-based archival file for macromolecular structures, *Eur. J. Biochem. 80*, 319−24.

BI060474W